ISBN: 978-3-95450-247-9 ISSN: 2673-5490 doi: 10.18429/JACoW-IPAC2024-MOPG37

SIMULATION STUDY FOR NANOMETER-SCALE MODULATION TRANSFER IN EMITTANCE EXCHANGE BEAMLINE

Gwanghui Ha*, Northern Illinois University, DeKalb, IL, USA
John Power, Argonne National Laboratory, Lemont, IL, USA
Aliaksei Halavanau, SLAC, Menlo Park, CA, USA
Gerard Andonian, James Rosenzweig, UCLA, Los Angeles, CA, USA

Abstract

Generating nanometer-scale density modulation has been pursued due to its potential for compact X-ray source applications. Realization of this nanometer modulation involves two key challenges: development of sub-micronscale momentum modulation method and conversion method to density modulation without quality degradation. Addressing the first challenge, emittance exchange (EEX) beamline is a promising candidate. Its unique capability of transverse-to-longitudinal phase space exchange makes it compatible with various modulators imparting either transverse or longitudinal modulations. This versatility allows us to find optimal radiators, addressing the second challenge. Study on degradation sources and their effects on the beam are underway to realize nanometer-scale modulation using EEX beamline. We present most recent results from our simulation study.

INTRODUCTION

Since the emittance exchange (EEX) was introduced [1, 2], various applications have been proposed [3–7] and demonstrated. The exchange of transverse and longitudinal phase space is a unique feature of the EEX beamline. It allows to apply any existing transverse manipulation methods to control the longitudinal phase space. One of attractive applications involves the generation of a longitudinal bunch train [5, 8–11]. Several experimental demonstrations have verified its feasibilty to generate mm-wave and microwave radiations. However, waves at the nanometer scale have never been experimentally demonstrated although EEX-based approaches are still considered an attractive approach.

Our collaboration aims to investigate a method for generating a bunch train compatible with radiation at the nanometer scale by extending our previous efforts and understanding of EEX-based longitudinal controls [3, 12–15]. This paper describes preliminary simulation results for the generation of a bunch train with a period of O(100) nm. Injector simulations were carried out using the Argonne Wakefield Accelerator's drive beamline. An EEX beamline was simulated using Elegant with artificially generated 6D Gaussian beam. 6D Gaussian beam was adopted to focus on the beam dynamics in the EEX beamline and avoid extra degradation originated from the injector. As the start of the research, we chose the initial modulation period of 1 μm to explore the challenges in a stepped approach. This initial modulation generates the final modulation period of 230 nm.

* gha@niu.edu

MODULATION REQUIREMENTS AND INJECTOR SIMULATION

The first step to generate a longitudinal density modulation via EEX is to impart either transverse density or divergence modulation. Here, we assume that a sinusoidal divergence modulation is imparted on the horizontal plane. One of the method's requirements is uncorrelated divergence. If the modulation amplitude is smaller than the uncorrelated divergence, particle behavior will be dominantly determined by their original divergence rather than a given modulation. Thus, the beam does not form a density modulation. Also, for given optics, the amplitude of the density modulation can be maximized when microbunches corresponding to each modulation period achieve maximum compression. This maximal compression can occur when the slope of each microbunch is $-R_{11}/R_{12}$ where R is a linear transfer matrix of the EEX beamline. When we apply sinusoidal modulation, the slope of each microbunch will be or close to Ak, where A is the modulation amplitude and k is the wave number. Thus, the modulation amplitude must satisfy the condition,

$$A = S_x/k = -\frac{2\pi R_{11}}{R_{12}\lambda}. \quad (1)$$

The modulation amplitude must be larger than the uncorrelated divergence. Therefore, the initial beam must satisfy the condition below.

$$\sigma_{x',uncorr} = \frac{\varepsilon_{nx}}{\beta\gamma\sigma_x} \leq A. \quad (2)$$

Another important factor to consider is the beam's other second moments and the charge. We simulated several different cases to determine reasonable initial beam assumptions for Elegant simulations. We chose 1 pC as the primary charge level to avoid significant degradation from CSR. Also, we simulated the AWA's drive beamline to identify achievable beam conditions. The scan results are summarized in Fig. 1. We selected parameters in Table 1 for Elegant simulations.

EEX BEAMLINE

The simulated EEX beamline consists of two identical doglegs and a transverse deflecting cavity (TDC) [3]. We added a fundamental mode cavity (FMC), sextupole magnets, and quadrupole magnets for specific purposes. Further details will be discussed in the following sections. The overall layout is displayed in Fig. 2, and the beamline setting is summarized in Table 2.

ISBN: 978-3-95450-247-9 ISSN: 2673-5490 doi: 10.18429/JACoW-IPAC2024-MOPG37

Table 1: Initial Condition for Elegant Simulations

Beam	Value	Modulation	Value
$\sigma_{x,y}$	300 µm	λ_{mod}	1 µm
$S_{x,y}$	0 m^{-1}	A_{mod}	1.2 µrad
$\varepsilon_{nx,ny}$	30 nm	λ_{fin}	230 nm
σ_z	100 µm		
S_z	0 m^{-1}		
σ_δ	5e-5		

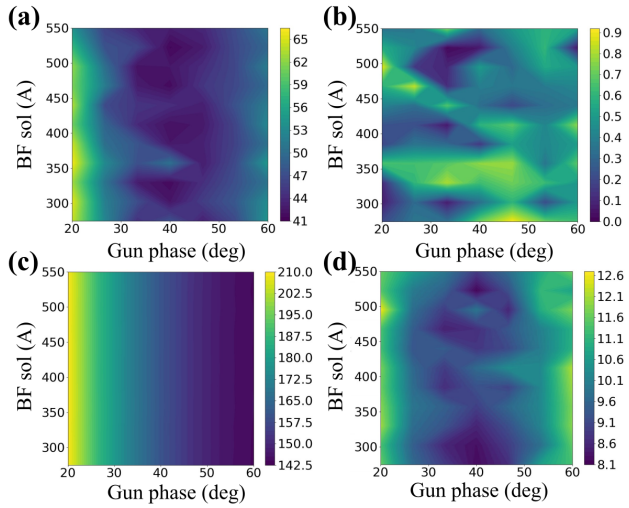

Figure 1: Injector simulation results. Bucking-Focusing (BF) solenoid, gun launching phase, and matching solenoid were scanned. The matching solenoid was optimized to minimize the transverse emittance. Each panel shows beam parameters at the end of the linac; (a) normalized x-emittance (nm), (b) rms x-size (mm), (c) normalized z-emittance (µm), and (d) rms z-length (µm).

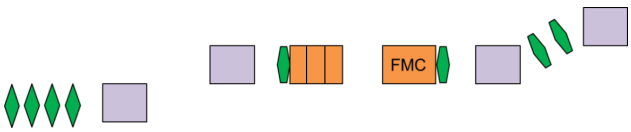

Figure 2: Schematic of the simulated EEX beamline.

Table 2: Beamline Parameters for EEX Simulation

Parameter	Value
Bending angle	10°
dipole-to-dipole	1.5 m
dip-to-cav & cav-to-cav	0.2 m
Quadrupole (K)	25, -18, 6, 13 m^{-2}
Sextupole (K$_2$)	-27, 89, -260, 273 m^{-3}
Dipole effective length	0.3 m
Quadrupole effective length	0.2 m
Sextupole effective length	0.2 m

LINEAR ORDER CORRECTION

Although the actual impact of each error source depends on how they act on the beam [12], most displacement errors will need to be controlled under a 100-nm level due to the expected final modulation period of 230 nm. Linear terms are the first factor that needs to be controlled. The original EEX beamline consists of two identical doglegs and a TDC. However, this design leaves unwanted non-zero diagonal terms in the transfer matrix, which originate from acceleration in TDC [16]. This effect is strong enough to wash out the entire modulations from the final current profile. Therefore, we adopted a fundamental mode cavity (FMC), which is a single-cell accelerating cavity, to compensate this effect [16].

SECOND ORDER CORRECTION

Elegant simulations assumed zero phase space slopes for all three planes. Thus, the major second-order terms were T_{511}, T_{533}, T_{515}, and T_{555}. To mitigate the second-order effects, four sextupole magnets were added along the beamline. Note that the locations of the sextupole magnets are not optimized, and the number of sextupole magnets and their locations could be changed.

Although sextupole magnets control second-order terms up to a certain level, clear limitations arise if the incident beam is too large. We used a 1 mm beam size in the transverse planes at the beginning. It significantly degraded the modulation quality. Thus, we decided to reduce the initial beam size based on the injector scan result. However, the one issue arising from reducing the beam size is the increase in uncorrelated divergence. It is necessary to increase the modulation amplitude to compensate the degradation from the increase in uncorrelated divergence. Since the modulation amplitude was matched to the ratio of R_{11} to R_{12}, the control of this ratio must be carried out with the reduction of the beam size. We added four quadrupoles upstream of the EEX beamline to keep R_{11} at the same level but decrease R_{12} to increase the ratio. The simulation results are displayed in Fig. 3. CSR is not included in this simulation.

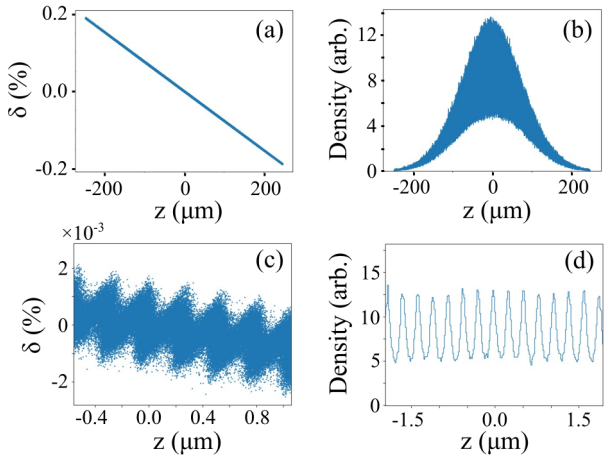

Figure 3: EEX simulation results with second-order correction.

ISBN: 978-3-95450-247-9 ISSN: 2673-5490 doi: 10.18429/JACoW-IPAC2024-MOPG37

CSR EFFECT AND ITS MITIGATION

Like other dispersive beamlines, the EEX beamline also faces challenges with CSR effects. The CSR significantly perturbs particles' final positions and washes out the modulation. The simulation results in Fig. 3 changed to the left column of Fig. 4 when we included the CSR in the simulation. The charge was 1 pC, and bins were set to 18,000 to consider the modulations. Although some modulation remained, the amplitude was significantly reduced, and it is impossible to see a clear modulation in the phase space.

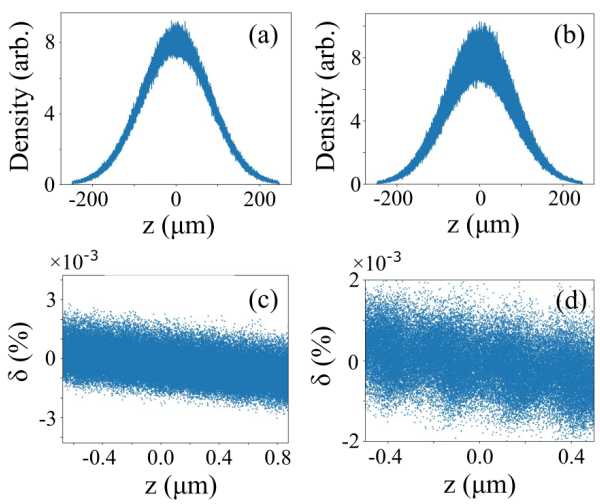

Figure 4: EEX simulation results with CSR effect.

We have confirmed that the CSR effect mostly depends on the macrobunch's length rather than the modulation. Additionally, we observed that the CSR effect from the first dogleg dominantly washed out the modulation because the bunch length was shorter in this region compared to the second dogleg. To address this issue, we decided to increase the initial bunch length to 400 μm. However, this adjustment disrupted the balance between second-order terms, so the sextupole magnets were reoptimized. The reoptimized results with σ_z =400 μm are displayed in panels (b) and (d) of Fig. 4. The modulation pattern became observable, and the modulation amplitude was almost doubled. Nonetheless, it is evident that further improvements are necessary.

From previous studies on the longitudinal shaping, it was confirmed that the CSR-related terms affecting the particles' final longitudinal positions always include R_{56} of the second dogleg as their coefficient [12]. Thus, Ref. [12] proposed the idea of an asymmetric dogleg, which reduces the bending angle of the second dogleg only. This method made significant changes to the shaping performance for high charges. We have applied this concept to assess its impact on the modulations.

The bending angle of the second dogleg was reduced to 10°, and the dipole-to-dipole distance was increased accordingly to match the dispersion to the exchange condition. The results are displayed in Fig. 5. Similar to shaping, the asymmetric dogleg successfully mitigated the CSR effects in the longitudinal direction. The modulation with CSR was slightly worse than the one without CSR. The final modulation with CSR showed a bunching factor of ~0.16. Here, the final modulation period is 230 nm.

For the experimental demonstration, we are considering radiation-based measurements to characterize the density modulation. The last simulation result is expected to generate 1×10^6-1×10^8 photons depending on the choice of a radiator (e.g., CTR and undulator radiation). This would be sufficient to diagnose the radiation.

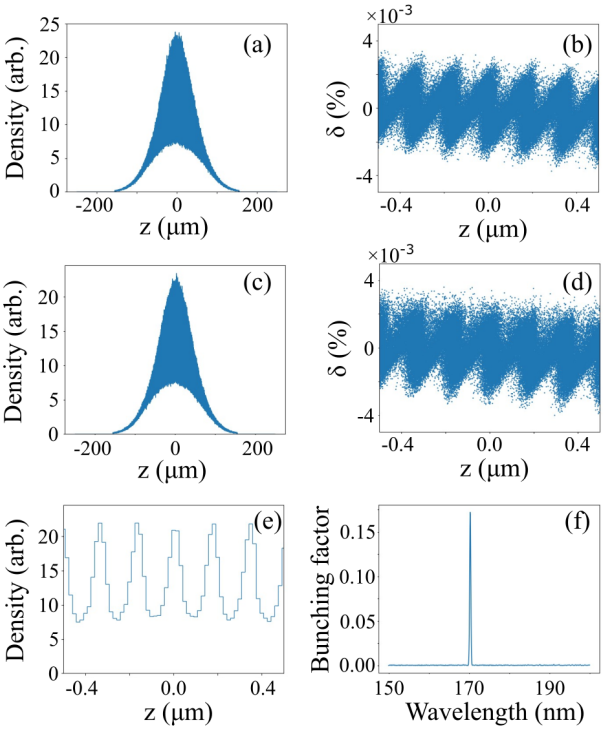

Figure 5: EEX simulation with asymmetric dogleg.

SUMMARY

We presented recent simulation results for generating submicron modulation using the EEX beamline. Injector parameters were determined based on simulations using the AWA facility's beamline. An artificial 6D Gaussian beam was generated using the injector scan results. Elegant simulations were conducted to explore each aberration source. Linear errors were corrected by the FMC, and second-order effects were mitigated by four sextupole magnets. Further adjustments were made to the transverse beam size and the bunch length in order to suppress the second-order effects and CSR effects more effectively. The final results with a charge of 1 pC showed observable modulation but clearly required improvement. Additionally, we applied previously studied asymmetric dogleg geometry to mitigate the CSR effect on the longitudinal plane. It significantly reduced the CSR effect on the modulation. CTR or undulator radiation from this density modulation is expected to generate sufficient photons characterizing the modulation.

ISBN: 978-3-95450-247-9 ISSN: 2673-5490 doi: 10.18429/JACoW-IPAC2024-MOPG37

REFERENCES

[1] M. Cornacchia and P. Emma, "Transverse to longitudinal emittance exchange," *Phys. Rev. ST Accel. Beams*, vol. 5, p. 084 001, 2002. doi:10.1103/PhysRevSTAB.5.084001

[2] P. Emma, Z. Huang, K.-J. Kim, and P. Piot, "Transverse-to-longitudinal emittance exchange to improve performance of high-gain free-electron lasers," *Phys. Rev. ST Accel. Beams*, vol. 9, p. 100 702, 2006. doi:10.1103/PhysRevSTAB.9.100702

[3] G. Ha *et al.*, "Precision control of the electron longitudinal bunch shape using an emittance-exchange beam line," *Phys. Rev. Lett.*, vol. 118, p. 104 801, 2017. doi:10.1103/PhysRevLett.118.104801

[4] T. Xu, M. Kuriki, P. Piot, and J. G. Power, "Damping-ring-free electron injector proposal for future linear colliders," *Phys. Rev. Accel. Beams*, vol. 26, p. 014 001, 1 2023. doi:10.1103/PhysRevAccelBeams.26.014001

[5] Y.-E. Sun *et al.*, "Tunable subpicosecond electron-bunch-train generation using a transverse-to-longitudinal phase-space exchange technique," *Phys. Rev. Lett.*, vol. 105, p. 234 801, 23 2010. doi:10.1103/PhysRevLett.105.234801

[6] G. Ha, "Emittance exchange with periphery cut for high-brightness beam," in *Proc. IPAC'23*, Venice, Italy, 2023, pp. 2763–2766. doi:10.18429/JACoW-IPAC2023-WEPA046

[7] B. E. Carlsten, K. A. Bishofberger, S. J. Russell, and N. A. Yampolsky, "Using an emittance exchanger as a bunch compressor," *Phys. Rev. ST Accel. Beams*, vol. 14, p. 084 403, 8 2011. doi:10.1103/PhysRevSTAB.14.084403

[8] W. S. Graves, F. X. Kärtner, D. E. Moncton, and P. Piot, "Intense superradiant x rays from a compact source using a nanocathode array and emittance exchange," *Phys. Rev. Lett.*, vol. 108, p. 263 904, 26 2012. doi:10.1103/PhysRevLett.108.263904

[9] A. Halavanau *et al.*, "Tailoring of an electron-bunch current distribution via space-to-time mapping of a transversely shaped, photoemission-laser pulse," *Phys. Rev. Accel. Beams*, vol. 22, p. 114 401, 11 2019. doi:10.1103/PhysRevAccelBeams.22.114401

[10] E. A. Nanni, W. S. Graves, and D. E. Moncton, "Nanomodulated electron beams via electron diffraction and emittance exchange for coherent x-ray generation," *Phys. Rev. Accel. Beams*, vol. 21, p. 014 401, 1 2018. doi:10.1103/PhysRevAccelBeams.21.014401

[11] G. Ha, M. E. Conde, J. G. Power, J. H. Shao, and E. E. Wisniewski, "Tunable Bunch Train Generation Using Emittance Exchange Beamline With Transverse Wiggler," in *Proc. IPAC'19*, Melbourne, Australia, May 2019, pp. 1612–1614. doi:10.18429/JACoW-IPAC2019-TUPGW089

[12] G. Ha, M. H. Cho, W. Gai, K.-J. Kim, W. Namkung, and J. G. Power, "Perturbation-minimized triangular bunch for high-transformer ratio using a double dogleg emittance exchange beam line," *Phys. Rev. Accel. Beams*, vol. 19, p. 121 301, 12 2016. doi:10.1103/PhysRevAccelBeams.19.121301

[13] Q. Gao *et al.*, "Observation of high transformer ratio of shaped bunch generated by an emittance-exchange beam line," *Phys. Rev. Lett.*, vol. 120, p. 114 801, 2018. doi:10.1103/PhysRevLett.120.114801

[14] R. Roussel *et al.*, "Single shot characterization of high transformer ratio wakefields in nonlinear plasma acceleration," *Phys. Rev. Lett.*, vol. 124, p. 044 802, 4 2020. doi:10.1103/PhysRevLett.124.044802

[15] J. Seok *et al.*, "Experimental demonstration of double emittance exchange toward arbitrary longitudinal beam phase-space manipulations," *Phys. Rev. Lett.*, vol. 129, p. 224 801, 22 2022. doi:10.1103/PhysRevLett.129.224801

[16] A. A. Zholents and M. S. Zolotorev, *A new type of bunch compressor and seeding of a short-wavelength coherent radiation.* ANL-APS-LS-327, 2011. doi:10.2172/1015557